Supplement of Atmos. Chem. Phys., 26, 11153–11169, 2026
https://doi.org/10.5194/acp-26-11153-2026-supplement

Atmospheric Chemistry and Physics Open Access

Supplement of

Exploring the hydrogen abstraction pathway in HOM formation from α-pinene photooxidation systems under varying NO conditions

Hui Wang et al.

Correspondence to: Defeng Zhao (dfzhao@fudan.edu.cn) and Sören R. Zorn (s.zorn@fz-juelich.de)

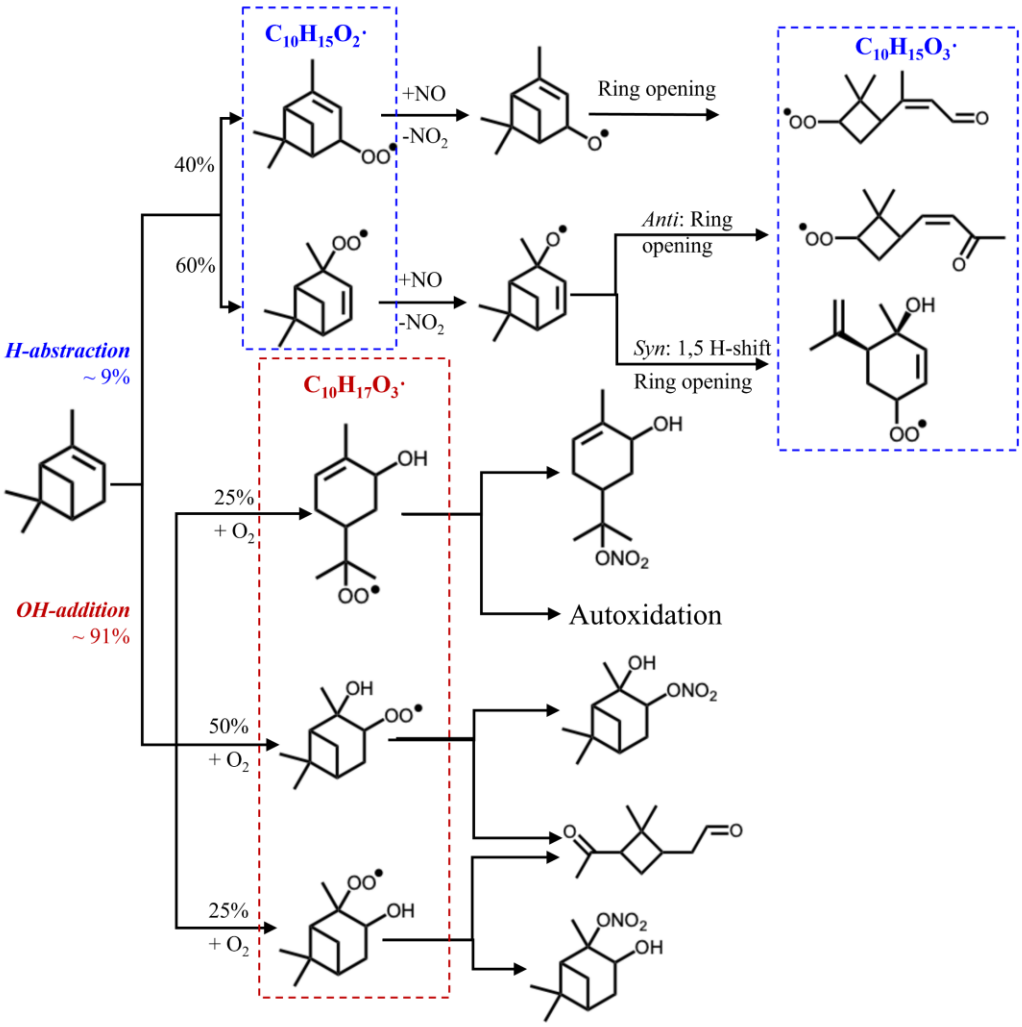

Figure S1. Formation pathways to form $C_{10}H_{15}O_3\cdot$ peroxy radicals through the H-abstraction channel and o form $C_{10}H_{17}O_3\cdot$ peroxy radicals through the OH-addition channel, derived from OH initiated α-pinene oxidation (Shen et al., 2022; Xu et al., 2019; Berndt et al., 2016).

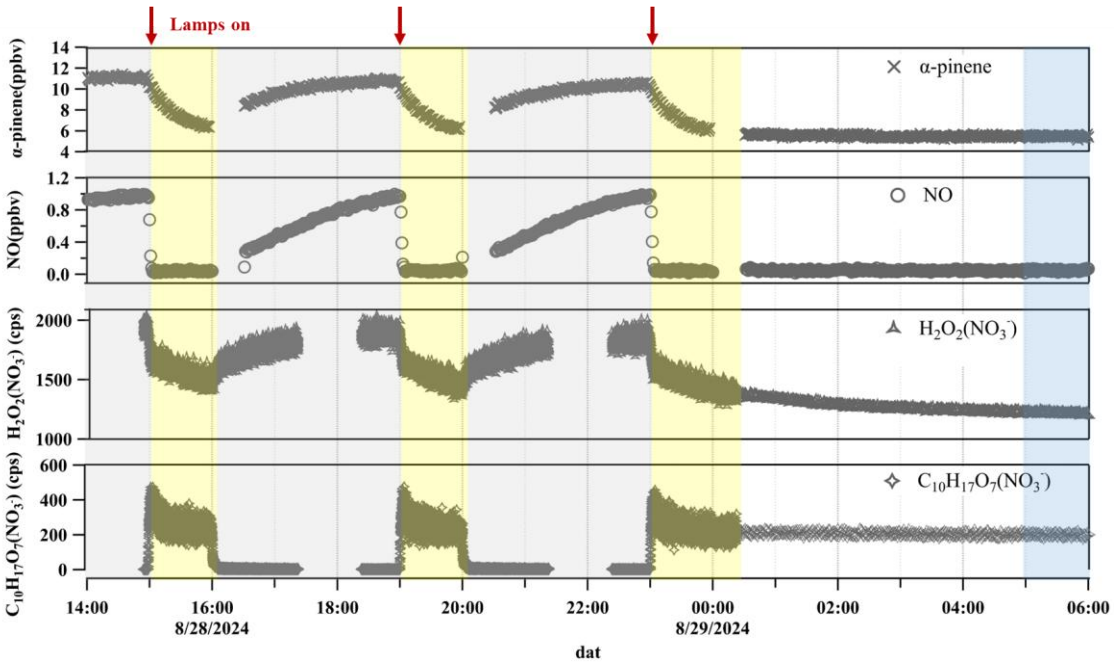

Figure S2. Time series of α-pinene concentration, NO concentration, along with normalized signal $H_2O_2(NO_3^-)$ and $C_{10}H_{17}O_7(NO_3^-)$. Three photooxidation experiments are presented, in which reactions were initialized by switching on UVC lamps when precursors are stable in dark conditions. In the third experiment, the lamps remain on for over six hours to allow the chamber to reach a steady-state condition.

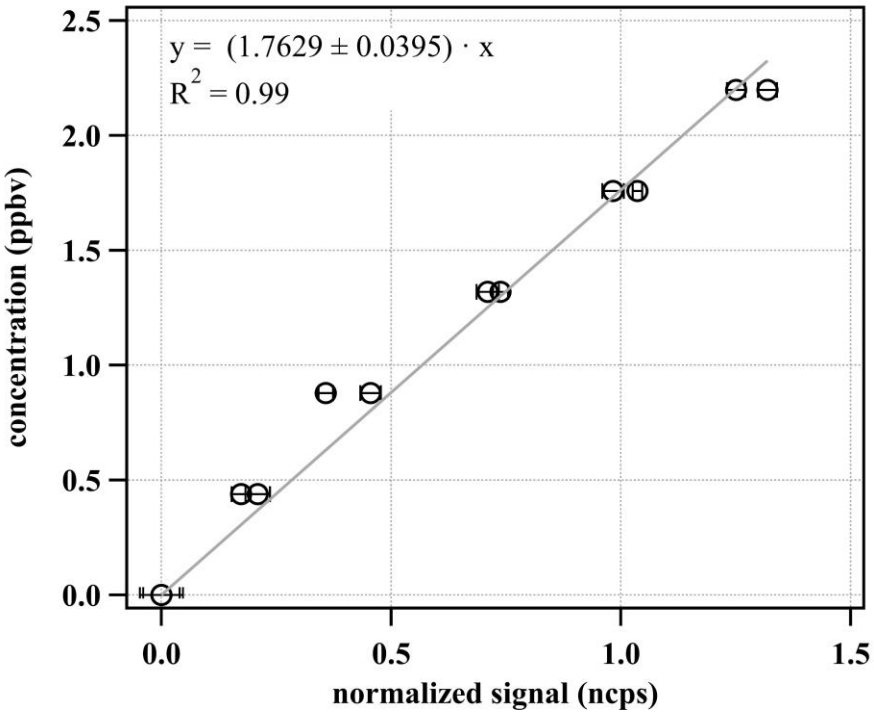

Figure S3. The calibration curve of pinonaldehyde in propylamine CIMS.

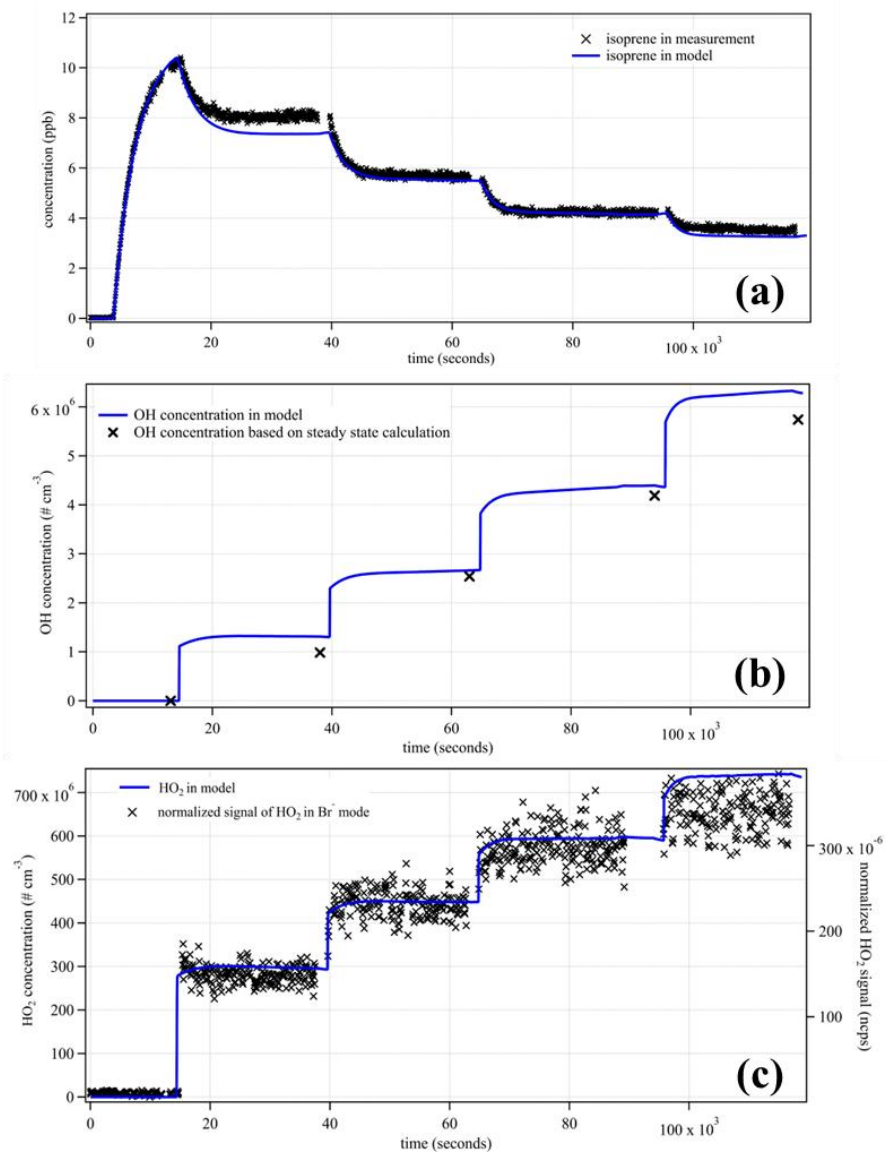

Figure S4. The time series of (a) measured isoprene (ppbv) and modeled isoprene (ppbv), (b) calculated concentration of OH radicals and modeled OH radicals, (c) normalized signal of $HO_2(Br^-)$ and HO_2 concentrations in model. The modeled data and measured data are presented in blue and dark, respectively.

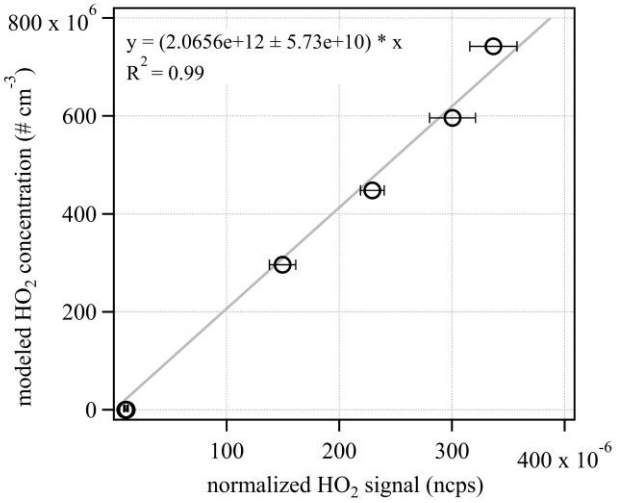

Figure S5. The modeled HO_2 concentrations are plotted versus normalized HO_2 signals, to obtain a calibration curve for HO_2 radicals.

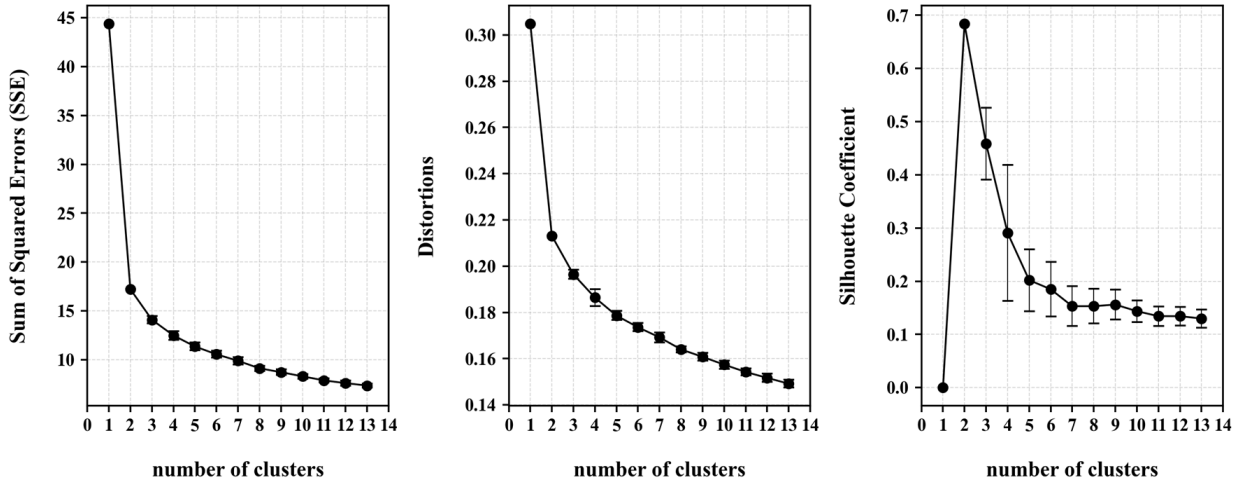

Figure S6. Values of selected clustering validity indices, sum of squared errors (SSE), distortions and Sihouette coefficients as a function of number of clusters from 1 to 13. The average of the results from 50 repetitions are shown in plots and error bars show the standard deviations.

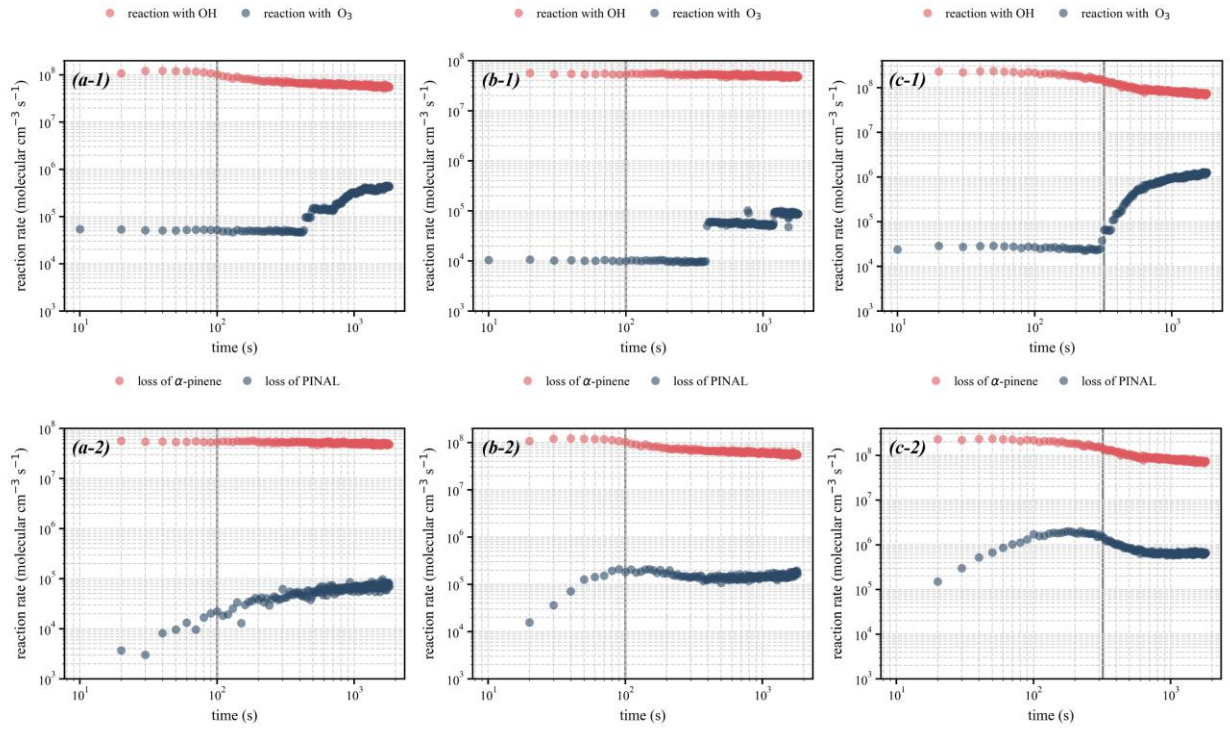

Figure S7. The upper panels (a-1 to c-1) compare the oxidation rates of α-pinene by OH and O_3 under NO-free, low-NO, and high-NO conditions, respectively. In each case, the relative contributions of OH- and O_3-initiated oxidation are shown. The lower panels (b-1 to c-1) compare the OH-initiated reaction losses of α-pinene and pinonaldehyde.

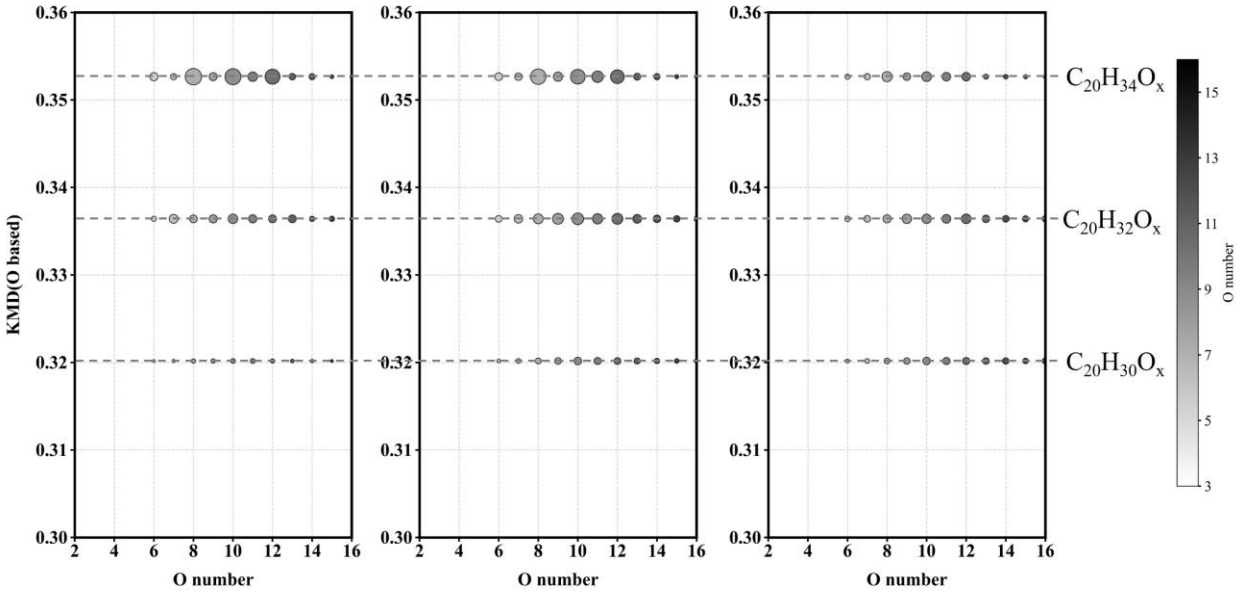

Figure S8. Kendrik Mass Defect (KMD, based on oxygen weight) of C_{20} accretion products as function of oxygen number are illustrated for without NO case (left), with low NO case (middle) and with high NO (right) case.

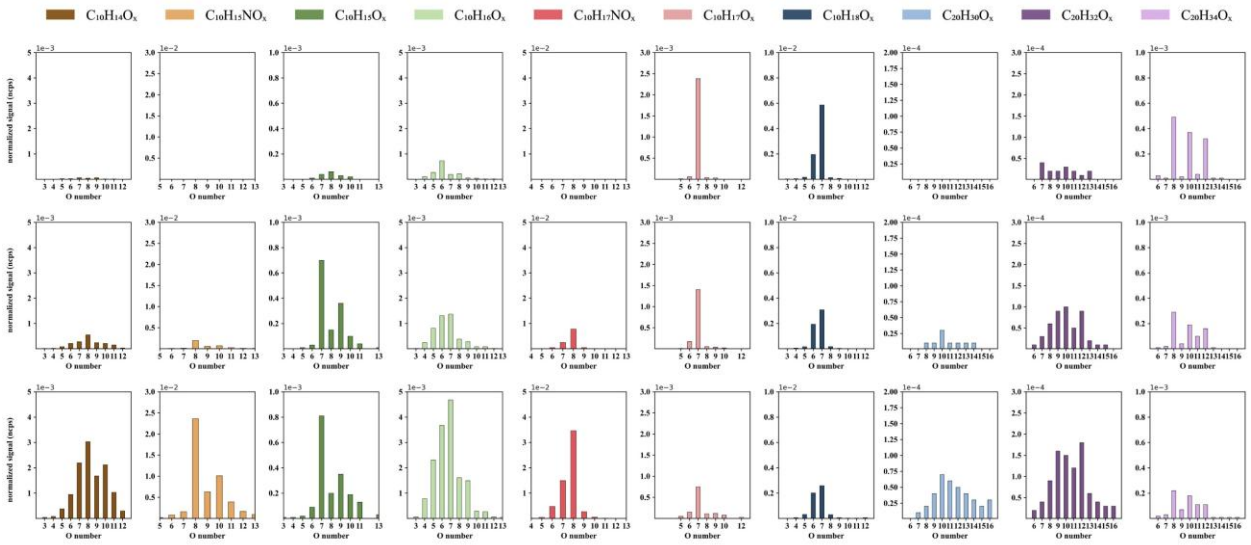

Figure S9. The normalized signals of major products are grouped into families are plotted versus oxygen number. From top to bottom, the three cases correspond to no-NO case, with low-NO case and with high-NO case, respectively. The data shown here are detected by nitrate CIMS.

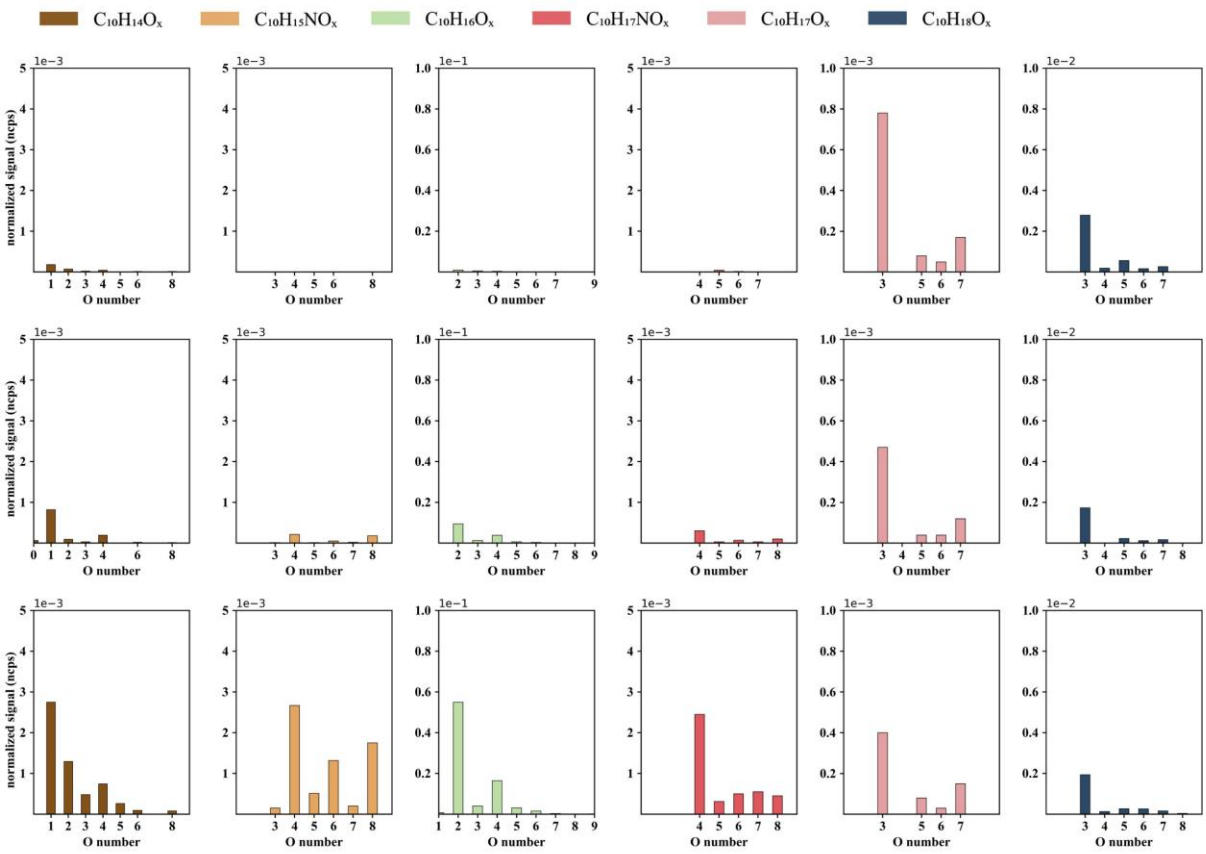

Figure S10. The normalized signals of major products are grouped into families are plotted versus oxygen number. From top to bottom, the three cases correspond to no-NO case, with low-NO case and with high-NO case, respectively. The data show only major monomers as measured by amine-CIMS.

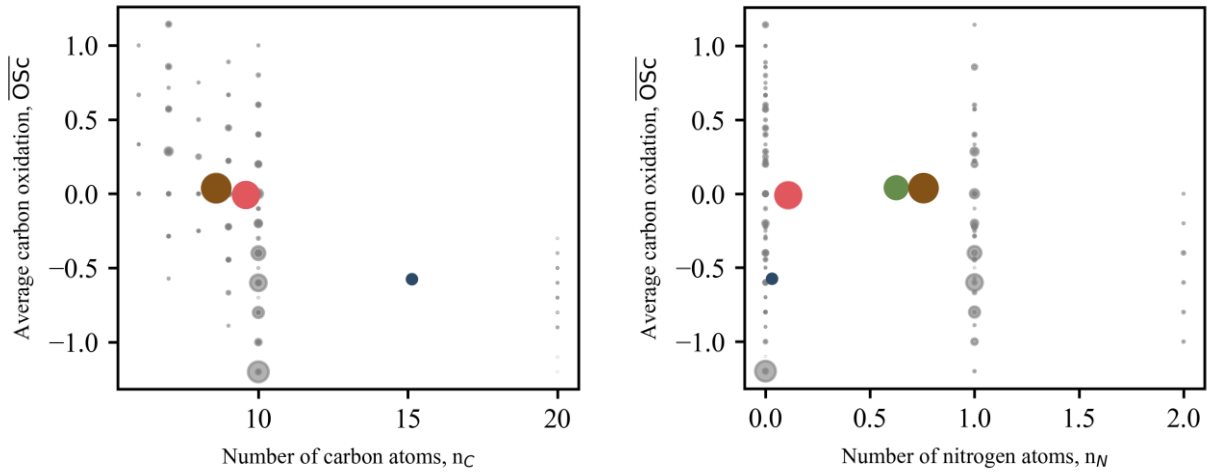

Figure S11. Average carbon oxidation state ($\overline{OSc}$) of four clusters obtained from fuzzy c-means clustering program are plotted as a function of average number of carbon atoms (left) and of average nitrogen atoms (right).

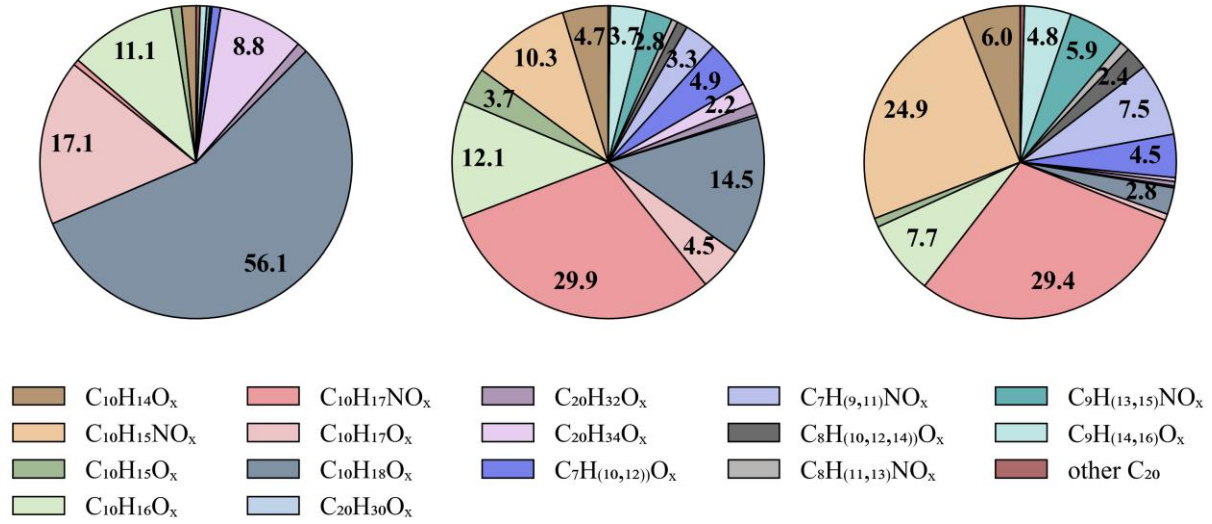

Figure S12. The pie plots illustrate the contribution of each family to the total compounds, from left to right showing NO-free case, with low-NO case and with high-NO case, respectively.

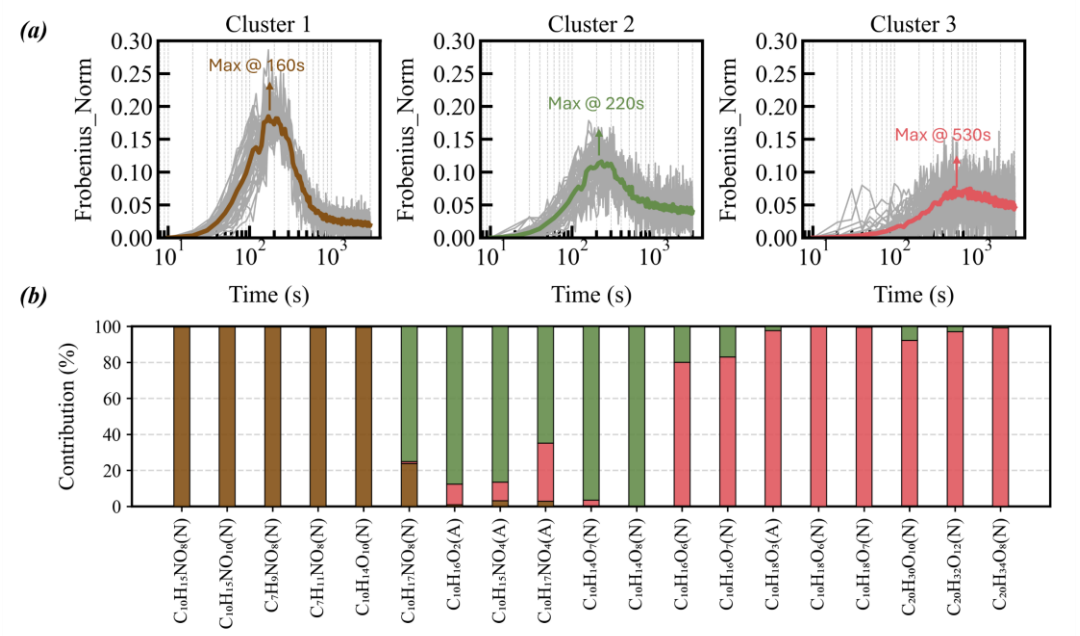

Figure S13. Results of fuzzy c-means clustering for three clusters for the dominant signals (156 in total) during early reaction stages of α-pinene photooxidation under high-NO condition are shown in panel ***(a)***. The time series of the cluster centers are displayed as colored solid lines, while individual contributing species are shown as gray lines. Panel ***(b)*** illustrates the cluster apportionment of selected major products detected in both nitrate-CIMS (N) and amine-CIMS (A).

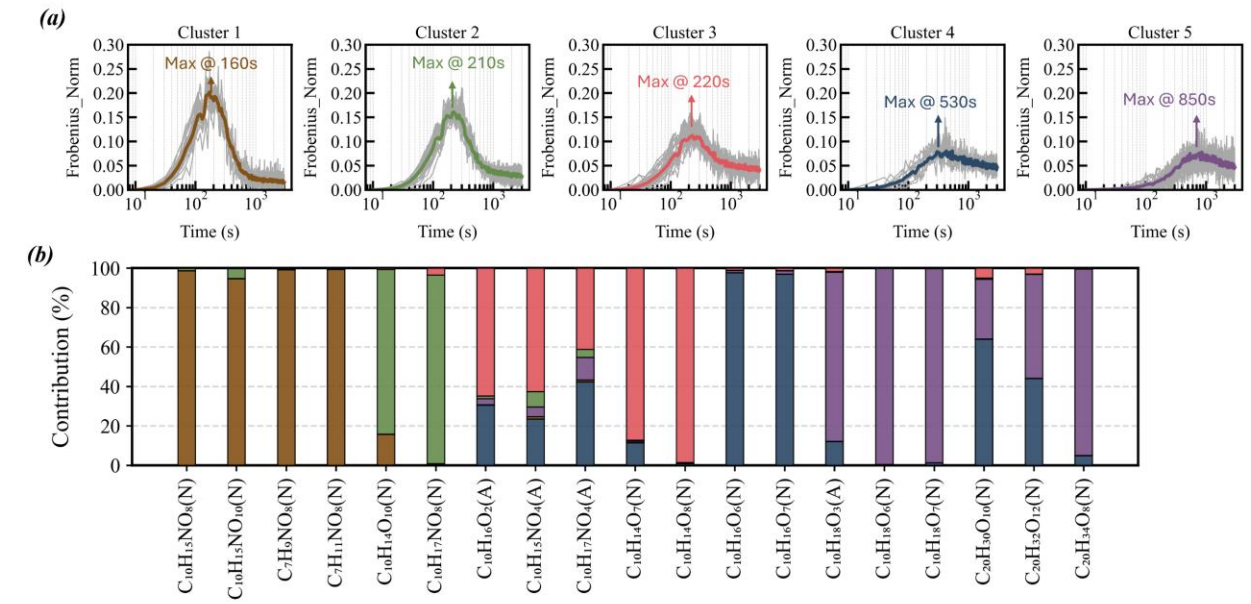

Figure S14. Results of fuzzy c-means clustering for five clusters for the dominant signals (156 in total) during early reaction stages of α-pinene photooxidation under high-NO condition are shown in panel ***(a)***. The time series of the cluster centers are displayed as colored solid lines, while individual species are shown as gray lines. Panel ***(b)*** illustrates the cluster apportionment of selected major products detected in both nitrate-CIMS (N) and amine-CIMS (A).

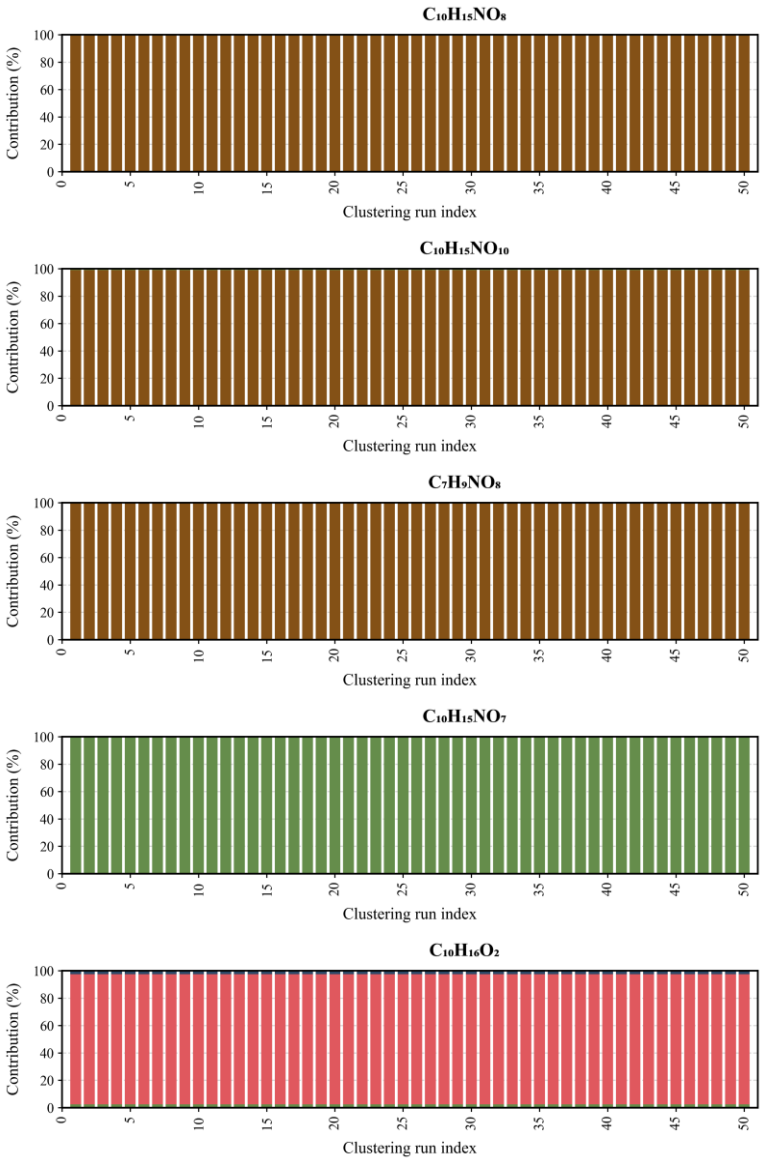

Figure S15 The results of 50 independent clustering runs using a four-cluster solution and random initialization are shown. The distributions of cluster assignments for key compounds are evaluated, including $C_{10}H_{15}NO_8(NO_3^-)$, $C_{10}H_{15}NO_{10}(NO_3^-)$, $C_7H_9NO_8(NO_3^-)$, $C_{10}H_{15}NO_7(NO_3^-)$, and $C_{10}H_{16}O_2(C_3H_7NH_3^+)$.

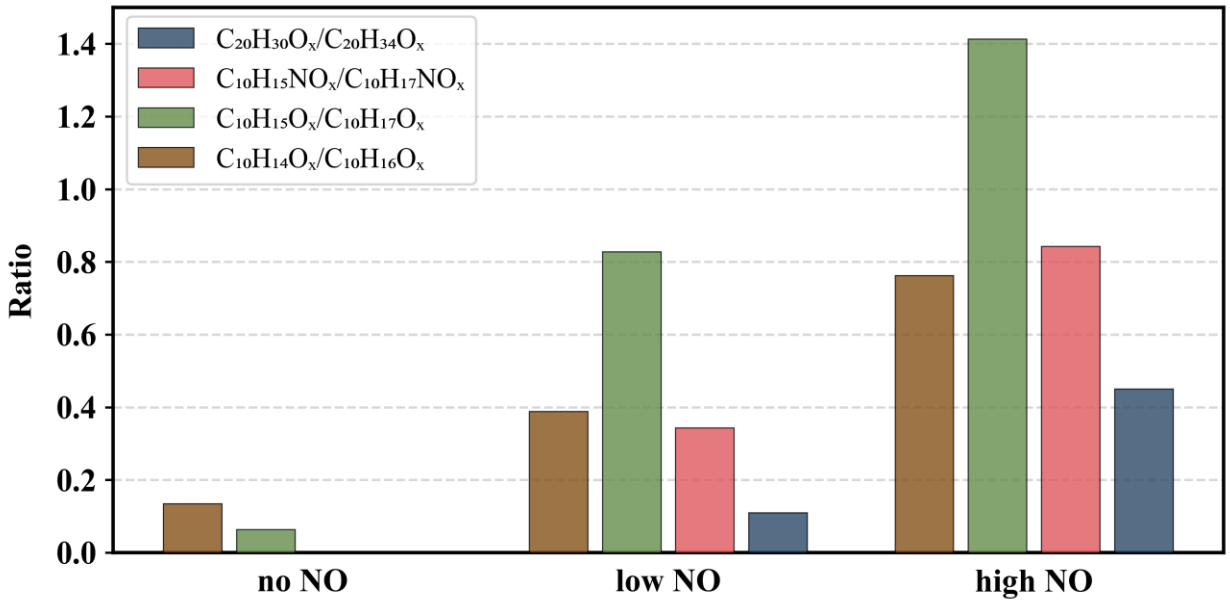

Figure S16. The bar plot represents ratios of product families potentially derived from H abstraction pathway to those potentially coming from OH addition pathway.

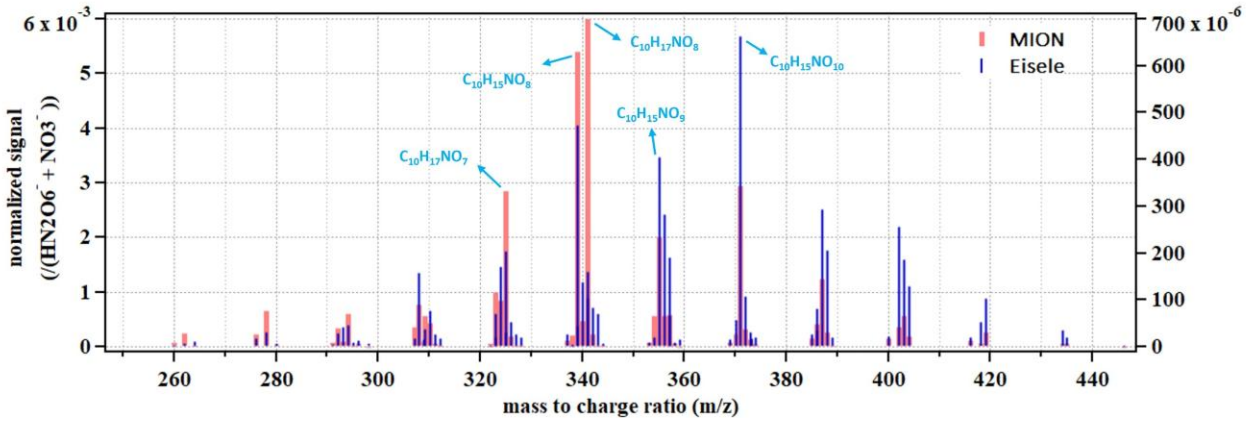

Figure S17. The signal of products derived from α-pinene oxidation with NO injection, detected by CIMS coupled with the MION (pink) and Eisele (blue) inlets.

References:

Berndt, T., Richters, S., Jokinen, T., Hyttinen, N., Kurten, T., Otkjaer, R. V., Kjaergaard, H. G., Stratmann, F., Herrmann, H., Sipila, M., Kulmala, M., and Ehn, M.: Hydroxyl radical-induced formation of highly oxidized organic compounds, NATURE COMMUNICATIONS, 7, 10.1038/ncomms13677, 2016.

Shen, H., Vereecken, L., Kang, S., Pullinen, I., Fuchs, H., Zhao, D., and Mentel, T. F.: Unexpected significance of a minor reaction pathway in daytime formation of biogenic highly oxygenated organic compounds, Science Advances, 8, eabp8702, doi:10.1126/sciadv.abp8702, 2022.

Xu, L., Moller, K. H., Crounse, J. D., Otkjaer, R. V., Kjaergaard, H. G., and Wennberg, P. O.: Unimolecular Reactions of Peroxy Radicals Formed in the Oxidation of alpha-Pinene and beta-Pinene by Hydroxyl Radicals, J Phys Chem A, 123, 1661-1674, 10.1021/acs.jpca.8b11726, 2019.